RAA 2015 Vol. **15** No. **7**, 986–992 doi: 10.1088/1674–4527/15/7/006
http://www.raa-journal.org *http://www.iop.org/journals/raa*

Research in Astronomy and Astrophysics

Effect of rapid evolution of magnetic tilt angle on a newborn magnetar's dipole radiation *

Ming Xu[1] and Yong-Feng Huang[2]

[1] Department of Physics, Jiangxi Science & Technology Normal University, Nanchang 330013, China; *xuming@nju.edu.cn*
[2] Department of Astronomy, Nanjing University, Nanjing 210093, China

Received 2014 August 18; accepted 2014 December 14

Abstract We study the electromagnetic radiation from a newborn magnetar whose magnetic tilt angle decreases rapidly. We calculate the evolution of the angular spin frequency, the perpendicular component of the surface magnetic field strength, and the energy loss rate through magnetic dipole radiation. We show that the spin-down of the magnetar experiences two stages characterized by two different timescales. The apparent magnetic field decreases with the decrease of the tilt angle. We further show that the energy loss rate of the magnetar is very different from that in the case of a fixed tilt angle. The evolution of the energy loss rate is consistent with the overall light curves of gamma-ray bursts which show a plateau structure in their afterglow stage. Our model supports the idea that some gamma-ray bursts with a plateau phase in their afterglow stage may originate from newborn millisecond magnetars.

Key words: magnetic fields — star: magnetars — gamma-ray bursts: general

1 INTRODUCTION

Magnetars such as Soft Gamma-Ray Repeaters and Anomalous X-ray Pulsars are highly magnetized neutron stars whose dipole magnetic field could be as high as $10^{14} - 10^{15}$ G (Mazets et al. 1979; Mereghetti & Stella 1995). Their internal magnetic fields could even be much higher than their external fields (Duncan & Thompson 1992; Paczynski 1992; Thompson & Duncan 1993).

Gamma-ray bursts (GRBs) are the most powerful stellar explosions in the universe. The relativistic internal and external shock model is the most successful mechanism to explain these violent events (Rees & Meszaros 1994; Piran 1999; Zhang 2007; Gehrels et al. 2009). Long GRBs could be due to the collapse of massive stars (Woosley 1993; Paczyński 1998; MacFadyen & Woosley 1999), and short GRBs could be connected with the coalescence of two compact objects (Eichler et al. 1989; Narayan et al. 1992; Gehrels et al. 2005; Nakar 2007).

A newborn magnetar with a millisecond rotational period could provide enough rotational energy to power the GRB ejecta (Usov 1992; Duncan & Thompson 1992). When the magnetar slowly spins down, the rotational energy released can provide a continuous energy-injection to the GRB jet and produce a plateau-like structure in the afterglow light curve (Dai & Lu 1998; Zhang & Mészáros

* Supported by the National Natural Science Foundation of China.

2001; Dai 2004) for both long and short GRBs (Fan & Xu 2006; Kobayashi & Zhang 2007; Yu & Dai 2007; Yu & Huang 2007; Xu et al. 2009; Yu et al. 2010; Dall'Osso et al. 2011; Bucciantini et al. 2012; Rowlinson et al. 2013).

To be eligible GRB progenitors, the magnetars should be born with millisecond rotational periods because the rotational energy needs to be as high as $\sim 10^{52}$ erg, which then can be comparable to the energy released in GRB explosions. Their dipole magnetic fields are also required to be higher than 10^{15} G (McKinney 2006; Bucciantini et al. 2007; Metzger et al. 2007, 2011), since a significant portion of the rotational energy should be released on the timescale of the GRB duration. On the other hand, in order to explain the relatively long-lasting shallow decays in the afterglow light curves, the magnetars should have a dipole magnetic field less than 10^{15} G (Fan & Xu 2006; Yu & Huang 2007; Xu et al. 2009; Yu et al. 2010; Dall'Osso et al. 2011). So, obvious conflicts exist in the requirements of the magnetic fields for magnetars as the central engines.

In this paper, we suggest that the contradiction of the magnetic field requirements could be solved by considering the evolution of the magnetic tilt angle of a magnetar. Due to the rapid decrease in the tilt angle, the perpendicular component of the magnetic dipole field at the surface of the magnetar also decreases rapidly. As a result, the apparent magnetic field can be very high in the beginning (i.e., the prompt GRB stage), but will be much lower at later times (i.e., the afterglow stage). Our scenario can explain well the overall light curves of those GRBs that have a plateau structure in their afterglow stage.

In Section 2, we describe the evolution of the tilt angle in our scenario. In Section 3, we present our detailed numerical results. Finally, Section 4 gives the conclusion and some brief discussions.

2 EVOLUTION OF MAGNETIC TILT ANGLE

Due to a strong magnetic field and rapid rotation, a newborn millisecond magnetar will radiate a huge amount of energy through magnetic dipole emission. This energy can be comparable to or even larger than the prompt energy release of GRBs and power the GRB ejecta (Usov 1992; Duncan & Thompson 1992; Dai & Lu 1998; Zhang & Mészáros 2001; Metzger et al. 2007). Through magnetic dipole radiation (Shapiro & Teukolsky 1983), the newborn magnetar loses energy at a rate of

$$\dot{E} = -\frac{2}{3c^3}|\ddot{m}|^2 \,, \tag{1}$$

where c is the speed of light in a vacuum, and m is the dipole moment of the magnetic field. We assume that the magnetar rotates at an angular frequency of Ω, and that the magnetic dipole moment m is oriented at an angle α with respect to the rotation axis.

Due to the rotation, the magnetic moment m is a function of time that can be described as

$$m = \frac{1}{2}B_{\rm p}R^3(e_{\parallel}\cos\alpha + e_{\perp}\,\sin\alpha\cos\,\Omega t + e'_{\perp}\sin\,\alpha\sin\,\Omega t)\,, \tag{2}$$

where $B_{\rm p}$ is the surface strength of the magnetic field at the magnetic pole, R is the radius of the magnetar, $e_{\parallel}$ is a unit vector parallel to Ω and $e_{\perp}$ and $e'_{\perp}$ are fixed mutually orthogonal unit vectors perpendicular to $e_{\parallel}$.

As a newly formed object, due to interaction between centrifugal deformation and the strong magnetic field, the deformation axis and the angular velocity vector will precess around the fixed axis of angular momentum (Cutler & Jones 2001; Dall'Osso et al. 2009). Due to gravitational wave damping of the magnetar wobble by internal viscous torques, the star becomes unstable and releases a huge amount of energy (Alpar & Sauls 1988; Cutler & Jones 2001; Stella et al. 2005; Dall'Osso et al. 2009; Ridley & Lorimer 2010). Along with magnetic deformation and gravitational wave damping, electromagnetic torque will also brake the rotation of the magnetar and rapidly decrease the tilt angle (Goldreich 1970; Cutler 2002). When the electromagnetic torque is taken into account,

the decaying timescale of the tilt angle is roughly equal to the characteristic spindown timescale of the magnetar. It is about several minutes for a strong dipolar field with strength of about 10^{16} G (Goldreich 1970; Shapiro & Teukolsky 1983; Cutler 2002).

To simplify, we assume that the tilt angle α is decaying at a constant rate with time as

$$\alpha = \alpha_0 - K \cdot t \,, \tag{3}$$

where α_0 is the initial tilt angle and K is a constant characterizing the rate of decrease. Assuming that the tilt angle stops changing at an angle $\alpha_{\rm end}$ at time $t_{\rm end}$, we can find $K = (\alpha_0 - \alpha_{\rm end})/t_{\rm end}$.

On the other hand, the radiation energy originates from the rotational kinetic energy of the magnetar, $E = \frac{1}{2} I \Omega^2$, where I is the moment of inertia of the magnetar. Thus the energy loss rate

$$\dot{E} = I\,\Omega\,\dot{\Omega}\,. \tag{4}$$

Due to the loss of the rotational energy, the magnetar slows down with time.

3 NUMERICAL CALCULATIONS AND RESULTS

In order to numerically calculate the evolution of the magnetic tilt angle, we first assume the following typical initial parameters: the surface dipolar magnetic field strength $B_{\rm p} = 1.0 \times 10^{16}$ G, the radius of the magnetar $R = 1.2 \times 10^6$ cm and the moment of inertia $I = 2.0 \times 10^{45}$ g cm^2. The initial spin period is assumed to be $P_0 = 1.0 \times 10^{-3}$ s, i.e., with an initial spin angular frequency $\Omega_0 = 2\pi/P_0 \approx 6.3 \times 10^3$ rad s^{-1}.

In this paper, we assume that the tilt angle α is decreasing at a constant rate with time. The initial tilt angle is assumed to be $\alpha_0 = \pi/3$ rad. It decreases at a constant rate to $\alpha_{\rm end} = 0.06$ rad within $t_{\rm end} = 100.0$ s. From Equation (3), we can get $K \approx 0.01$ rad s^{-1}.

For the fixed tilt angle scenario, we can define a characteristic timescale (Shapiro & Teukolsky 1983) by

$$T_{\rm c} = \frac{6Ic^3}{B_{\rm p}^2 R^6 \sin^2\alpha \Omega_{\rm i}^2}\,, \tag{5}$$

where $\Omega_{\rm i}$ is the initial angular frequency. Thus, for a fixed tilt angle of $\alpha = \alpha_0 = \pi/3$ rad, the characteristic timescale is about $T_{\rm c} = 36.8$ s, and it is about 7.7×10^3 s for a fixed tilt angle of $\alpha = \alpha_{\rm end} = 0.06$ rad.

With the above initial parameters, we can calculate the aforementioned differential equations. The solid curve in Figure 1 shows the evolution of the angular frequency of a magnetar for the scenario with a rapid decrease in the magnetic tilt angle. For comparison, we also show the spin-down evolution of magnetars without tilt angle evolution in Figure 1.

As shown by the solid curve in Figure 1, in our scenario, the spin-down occurs in two stages as the tilt angle decreases. At first, Ω decreases along the dashed curve with a characteristic timescale of about 37 s. Because of the rapid decrease of α, the evolution of Ω deviates from the dashed line after about 30 s. After 100 s, the tilt angle stops evolving and becomes fixed at $\alpha_{\rm end} = 0.06$ rad, and Ω also evolves to about 3.4×10^3 rad s^{-1}. Then, Ω decreases with a new characteristic timescale of about 2.6×10^4 s. Finally, Ω decreases along the dotted curve.

Figure 2 illustrates the evolution of the perpendicular component of the dipole magnetic field, i.e., apparent magnetic field $B_\perp = B_{\rm p}\sin\alpha$. We have assumed that the newborn magnetar has a dipole magnetic field of $B_{\rm p} = 1.0 \times 10^{16}$ G, thus we initially have $B_\perp = B_{\rm p}\sin(\pi/3) \doteq 8.7 \times 10^{15}$ G. This value is shown as a dashed line, i.e., for the case of a fixed tilt angle of $\alpha = \alpha_0 = \pi/3$ rad. Within 100.0 s, the tilt angle rapidly decreases to $\alpha_{\rm end} = 0.06$ rad, and $B_\perp$ decays accordingly to about 6.0×10^{14} G. The dotted line shows this magnetic field value for a fixed tilt angle of 0.06 rad. The overall evolution of $B_\perp$ in our scenario is shown as the solid curve. We

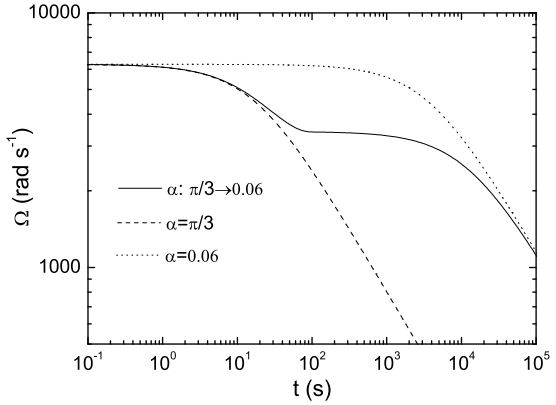

Fig. 1 Evolution of the angular velocity of magnetars. The solid curve corresponds to our model with the tilt angle decreasing from $\pi/3$ rad to 0.06 rad within 100.0 s. The dashed and dotted curves correspond to magnetars with fixed tilt angles of $\pi/3$ rad and 0.06 rad, respectively.

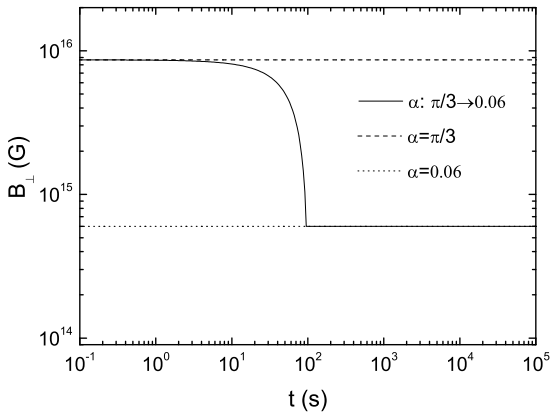

Fig. 2 The evolution of the perpendicular component of the dipole magnetic field ($B_{\perp} = B_{\rm p}\sin\alpha$). The solid curve corresponds to our model with a decreasing tilt angle. The dashed and dotted lines are $B_{\perp}$ for fixed tilt angles of $\pi/3$ and 0.06 rad, respectively.

see that the apparent magnetic field decays rapidly from 8.7×10^{15} G to 6.0×10^{14} G due to the evolution of the tilt angle.

Evolution of the energy loss rate of the magnetar is shown in Figure 3. The dashed and dotted curves are for the cases of fixed tilt angles of $\pi/3$ and 0.06 rad, respectively. As shown in Figure 3, the evolution of the energy loss rate of the magnetar in our scenario can be divided into two stages. At first, $\dot{E}$ decays along the dashed curve, similar to the evolution of $\dot{E}$ for the fixed scenario of $\pi/3$ rad. With the rapid decrease of the magnetic tilt angle, the magnetar then releases energy slower than in the fixed tilt angle scenario, thus the evolution deviates from the dashed curve. One hundred seconds later, the tilt angle terminates at $\alpha_{\rm end} = 0.06$ rad. Within this period, $\dot{E}$ evolves from the initial value of about 2.2×10^{51} erg s^{-1} to about 9.0×10^{47} erg s^{-1}. Then, the evolution of $\dot{E}$ enters the second stage. Finally, $\dot{E}$ decreases along the dotted curve.

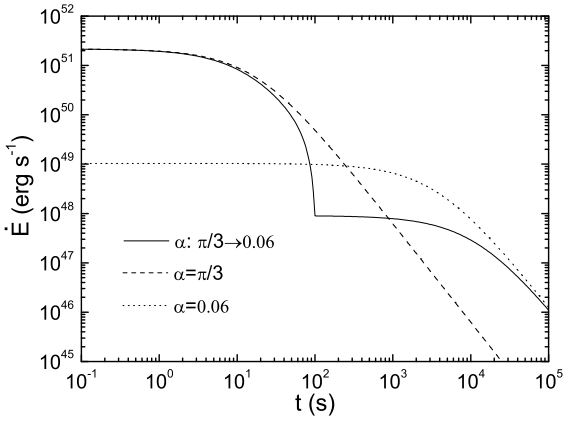

Fig. 3 Evolution of the energy loss rate ($\dot{E}$) of magnetars during the spin-down. The solid curve corresponds to our model with a decreasing tilt angle. The dashed and dotted curves correspond to the evolution of $\dot{E}$ for fixed tilt angles of $\pi/3$ and 0.06 rad, respectively.

4 CONCLUSIONS AND DISCUSSION

The analysis in this paper shows that the energy loss rate of a newborn magnetar with a rapidly decreasing magnetic tilt angle is very different from that of the scenario with a fixed tilt angle. Because of the decreasing magnetic tilt angle, the spin-down of the magnetar is characterized by two different timescales. Although the magnetic field strength of the magnetar does not change during the process, the apparent magnetic field $B_{\perp}$ decreases by more than one order of magnitude. The energy loss rate due to magnetic dipole radiation also experiences two stages.

For a normal neutron star, the magnetic tilt angle usually evolves on a timescale of about several million years due to the joint effect of the spin and strong gravity (Zhang et al. 1998). However, for a newborn magnetar, the superstrong magnetic field will lead to a significant deformation. Together with a millisecond rotation, it could be a strong source of gravitational wave emission (Ioka 2001; Palomba 2001), which naturally leads to a decrease in the tilt angle. Additionally, the electromagnetic torque also tends to align the magnetic axis with the rotation axis (Goldreich 1970; Alpar & Sauls 1988; Cutler & Jones 2001; Cutler 2002; Dall'Osso et al. 2009). In our study, we have assumed a realistic surface magnetic field of about 10^{16} G (Stella et al. 2005; Lazzati et al. 2005; Nakar et al. 2006; Popov & Stern 2006). Considering the differential rotation and the internal magnetic configuration, the internal field should be significantly higher (Ruderman 1991; Thompson & Duncan 1993; Duncan 1998) and could be as large as $\sim 10^{17}$ G (Mallick & Schramm 2014). It can naturally result in a remarkable deformation and make the magnetic tilt angle decrease significantly in about 100 s.

Due to the rapid decrease of the magnetic tilt angle, the magnetar slows down in an unusual way. The braking behavior differs markedly from that caused by normal magnetic dipole radiation. As a result, the braking index ($n = \Omega\ddot{\Omega}/\dot{\Omega}^2$) will deviate from 3. This mechanism could possibly explain the abnormal braking index observed in many pulsars (Lyne et al. 1996; Marshall et al. 2004; Archibald et al. 2013).

From our analysis, we find that the apparent magnetic field decays rapidly when the magnetic tilt angle decreases. However, the strength of the dipole magnetic field itself does not change. It naturally provides a solution to the controversial requirements for the magnetic field mentioned above, which were previously explained as being due to some special mechanisms associated with magnetic field decay (Pacini 1969; Colpi et al. 2000; Pons et al. 2009).

The energy loss rate experiences a two-stage evolution. It changes from the initial value of 2.2×10^{51} erg s^{-1} to about 9.0×10^{47} erg s^{-1} within 100.0 s. At first, the energy loss rate is large enough to power the GRB prompt emission. At the second stage, the energy loss rate can provide necessary energy injection for the GRB fireball and power the afterglow emission (Zhang 2007; Gehrels et al. 2009; Sultana et al. 2012; D'Avanzo et al. 2012). Comparing the evolution curve of the energy loss rate with the overall GRB light curves (from the prompt emission to the afterglow stage, Zhang et al. 2006; Nousek et al. 2006), we find that they are very similar. So, we argue that some GRBs with a plateau phase in their afterglow stage may actually happen as follows. Initially, the newborn millisecond magnetar releases a huge amount of energy to launch powerful ejecta to produce a burst. This corresponds to the prompt emission phase. As the tilt angle rapidly decreases, the energy released from the magnetar also reduces markedly. Since the energy loss rate is no longer powerful enough to maintain the burst, a steep decay phase will naturally appear in the GRB light curve. When the tilt angle finally becomes stable, the energy loss rate enters a new stage. It decreases slowly on a timescale of several thousand seconds and energy is continuously injected into the fireball. This stage corresponds to the shallow decay phase in the GRB afterglow light curve. Finally, the energy injection comes to an end when most of the rotational energy in the magnetar is consumed. Then the afterglow enters its normal decay phase.

It has been widely argued that the progenitors of GRBs could be collapsars (Woosley 1993; Paczyński 1998; MacFadyen & Woosley 1999), merging compact objects (Eichler et al. 1989; Narayan et al. 1992; Gehrels et al. 2005; Nakar 2007), or newborn magnetars (Usov 1992; Thompson 1994; Metzger et al. 2011). Our study supports the idea that those GRBs with a plateau phase in the afterglow light curve may originate from newborn millisecond magnetars (Xu & Huang 2012).

Acknowledgements We would like to thank the anonymous referee for their helpful suggestions. We also thank Z. G. Dai and Y. Z. Fan for stimulating discussions. This work was supported by the National Basic Research Program of China (973 program, Grant No. 2014CB845800), and by the National Natural Science Foundation of China (Grant Nos. 11203020, 11473012 and 11033002), and Jiangxi Province Science Foundation for Youths (Grant No. 20151BAB216028).

References

Alpar, M. A., & Sauls, J. A. 1988, ApJ, 327, 723
Archibald, R. F., Kaspi, V. M., Ng, C.-Y., et al. 2013, Nature, 497, 591
Bucciantini, N., Metzger, B. D., Thompson, T. A., & Quataert, E. 2012, MNRAS, 419, 1537
Bucciantini, N., Quataert, E., Arons, J., Metzger, B. D., & Thompson, T. A. 2007, MNRAS, 380, 1541
Colpi, M., Geppert, U., & Page, D. 2000, ApJ, 529, L29
Cutler, C. 2002, Phys. Rev. D, 66, 084025
Cutler, C., & Jones, D. I. 2001, Phys. Rev. D, 63, 024002
Dai, Z. G. 2004, ApJ, 606, 1000
Dai, Z. G., & Lu, T. 1998, A&A, 333, L87
Dall'Osso, S., Shore, S. N., & Stella, L. 2009, MNRAS, 398, 1869
Dall'Osso, S., Stratta, G., Guetta, D., et al. 2011, A&A, 526, A121
D'Avanzo, P., Salvaterra, R., Sbarufatti, B., et al. 2012, MNRAS, 425, 506
Duncan, R. C. 1998, ApJ, 498, L45
Duncan, R. C., & Thompson, C. 1992, ApJ, 392, L9
Eichler, D., Livio, M., Piran, T., & Schramm, D. N. 1989, Nature, 340, 126
Fan, Y.-Z., & Xu, D. 2006, MNRAS, 372, L19
Gehrels, N., Ramirez-Ruiz, E., & Fox, D. B. 2009, ARA&A, 47, 567
Gehrels, N., Sarazin, C. L., O'Brien, P. T., et al. 2005, Nature, 437, 851
Goldreich, P. 1970, ApJ, 160, L11

Ioka, K. 2001, MNRAS, 327, 639
Kobayashi, S., & Zhang, B. 2007, ApJ, 655, 973
Lazzati, D., Ghirlanda, G., & Ghisellini, G. 2005, MNRAS, 362, L8
Lyne, A. G., Pritchard, R. S., Graham-Smith, F., & Camilo, F. 1996, Nature, 381, 497
MacFadyen, A. I., & Woosley, S. E. 1999, ApJ, 524, 262
Mallick, R., & Schramm, S. 2014, Phys. Rev. C, 89, 045805
Marshall, F. E., Gotthelf, E. V., Middleditch, J., Wang, Q. D., & Zhang, W. 2004, ApJ, 603, 682
Mazets, E. P., Golentskii, S. V., Ilinskii, V. N., Aptekar, R. L., & Guryan, I. A. 1979, Nature, 282, 587
McKinney, J. C. 2006, MNRAS, 368, 1561
Mereghetti, S., & Stella, L. 1995, ApJ, 442, L17
Metzger, B. D., Giannios, D., Thompson, T. A., Bucciantini, N., & Quataert, E. 2011, MNRAS, 413, 2031
Metzger, B. D., Thompson, T. A., & Quataert, E. 2007, ApJ, 659, 561
Nakar, E. 2007, Phys. Rep., 442, 166
Nakar, E., Gal-Yam, A., Piran, T., & Fox, D. B. 2006, ApJ, 640, 849
Narayan, R., Paczynski, B., & Piran, T. 1992, ApJ, 395, L83
Nousek, J. A., Kouveliotou, C., Grupe, D., et al. 2006, ApJ, 642, 389
Pacini, F. 1969, Nature, 224, 160
Paczynski, B. 1992, Acta Astronomica, 42, 145
Paczyński, B. 1998, ApJ, 494, L45
Palomba, C. 2001, A&A, 367, 525
Piran, T. 1999, Phys. Rep., 314, 575
Pons, J. A., Miralles, J. A., & Geppert, U. 2009, A&A, 496, 207
Popov, S. B., & Stern, B. E. 2006, MNRAS, 365, 885
Rees, M. J., & Meszaros, P. 1994, ApJ, 430, L93
Ridley, J. P., & Lorimer, D. R. 2010, MNRAS, 404, 1081
Rowlinson, A., O'Brien, P. T., Metzger, B. D., Tanvir, N. R., & Levan, A. J. 2013, MNRAS, 430, 1061
Ruderman, M. 1991, ApJ, 366, 261
Shapiro, S. L., & Teukolsky, S. A. 1983, Black Holes, White Dwarfs, and Neutron Stars: The Physics of Compact Objects (New York: Wiley-Interscience)
Stella, L., Dall'Osso, S., Israel, G. L., & Vecchio, A. 2005, ApJ, 634, L165
Sultana, J., Kazanas, D., & Fukumura, K. 2012, ApJ, 758, 32
Thompson, C. 1994, MNRAS, 270, 480
Thompson, C., & Duncan, R. C. 1993, ApJ, 408, 194
Usov, V. V. 1992, Nature, 357, 472
Woosley, S. E. 1993, ApJ, 405, 273
Xu, M., & Huang, Y. F. 2012, A&A, 538, A134
Xu, M., Huang, Y.-F., & Lu, T. 2009, RAA (Research in Astronomy and Astrophysics), 9, 1317
Yu, Y., & Huang, Y.-F. 2007, ChJAA (Chin. J. Astron. Astrophys.), 7, 669
Yu, Y.-W., Cheng, K. S., & Cao, X.-F. 2010, ApJ, 715, 477
Yu, Y. W., & Dai, Z. G. 2007, A&A, 470, 119
Zhang, B. 2007, ChJAA (Chin. J. Astron. Astrophys.), 7, 1
Zhang, B., Fan, Y. Z., Dyks, J., et al. 2006, ApJ, 642, 354
Zhang, B., & Mészáros, P. 2001, ApJ, 552, L35
Zhang, C. M., Cheng, K. S., & Wu, X. J. 1998, A&A, 332, 569